PPS®1350-G Performance assessment with permanent magnets

IEPC-2011-119

Presented at the 32nd International Electric Propulsion Conference,
Wiesbaden • Germany
September 11 – 15, 2011

V. Vial[*], L. Godard[†] and N. Cornu[‡]
Snecma, Safran Group, Space Engines Division, 27200 Vernon, France

and

E. Coulaud[§] and D. Arrat[**]
Centre National d'Etudes Spatiales, 31000 Toulouse, France

Abstract: Optimization of Hall-Effect thrusters design represents numerous scientific, technical and commercial challenges. In order to test the feasibility of future options a technology demonstrator of the PPS®1350-G thruster, namely the PPS®1350-DT, was manufactured. The paper presents the comprehensive study carried out on the magnetic architecture specificities. First magnetic modelling were performed to design permanent magnets on the base of the PPS®1350-G reference magnetic topology. Second a firing test campaign aimed at characterizing the demonstrator operation both with coils and magnets around the nominal operating point: the performance in the magnet configuration complies with the reference one. The paper finally presents the benefits of a PPS®1350 optimized with permanent magnets.

Nomenclature

B	=	magnetic field
Brem	=	remanence
B_r	=	radial magnetic component
Br_{max}	=	maximal radial magnetic component at the channel exit
B_z	=	axial magnetic component
E	=	electric field
Id	=	Discharge current
Idosc	=	Discharge current oscillation level
Isp	=	Specific impulse
L_c	=	Discharge channel length
$r_{Le,i}$	=	Larmor radius for electrons, ions
T_{max}	=	Magnet maximal functional temperature
Ucrp	=	Cathode retarding potential

[*] Ph.D, R&D Engineer, Plasma Propulsion Department, vanessa.vial@snecma.fr
[†] Senior Engineer, Plasma Propulsion Department, laurent.godard@snecma.fr
[‡] Chief Engineer, Head of the Plasma Propulsion Department, nicolas.cornu@snecma.fr
[§] Engineer, Electric Propulsion Department, emilie.coulaud@cnes.fr
[**] Chief Engineer, Head of the Electric Propulsion Department, denis.arrat@cnes.fr

μr = magnetic permeability of the material

I. Introduction

THE development of electric propulsion systems based on Hall Effect Thrusters (HET) expanded significantly since the first demonstration in flight on the soviet satellite Meteor in 1972. The reliability and performance of 1.5kW-class HET have widely been demonstrated on-board numerous spacecrafts, particularly on communication satellites. As a result a significant heritage in terms of HET physics and technologies has been produced worldwide for more than 40 years.

In Snecma a wide experience has been acquired since 1992 through numerous research activities carried out on HET from few hundreds of watts[1] up to tens of kilowatts.[2] The obtained results participate to the improvement of the 1.5kW-class PPS®1350-G competitiveness.

A. HET operating principle

Figure 1 shows the specific electric and magnetic architecture of a HET that generates the so-called **ExB** and Hall current. This crossed electric and magnetic field topology enables both gas ionization and ions ejection in a reduced area around the thruster exit plane.

B field is chosen such as the electron axial mobility is reduced in the exit plane, where the potential drop is thus mainly concentrated. The local **E** field accelerates ions to very high speed while Hall current ensures efficient ionization of the supplied gas.

Xenon is usually chosen as propellant because of its high atomic mass and low ionization energy, enabling to reach *Isp* and efficiency of more than 1500s and 50% respectively.

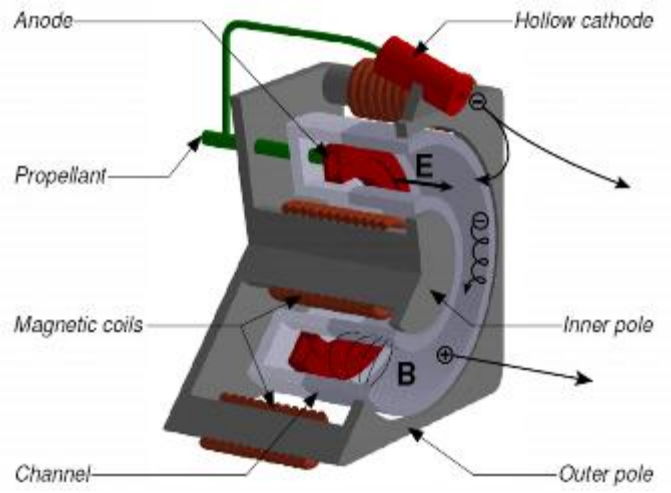

Figure 1. Sketch of a Hall Effect Thruster

B. Magnetic circuit architecture

1. Constraints and Challenges

The magnetic architecture is a key point in the design of a HET. In order to optimize both the ionization and acceleration processes, and in turn the thruster performance, the magnetic circuit must be designed to generate a very specific magnetic field. Basically **B** field must be chosen such as in the exit plane of the discharge chamber:

$$r_{Le} < L_c < r_{Li} \tag{1}$$

where r_{Le} and r_{Li} are respectively the Larmor radius for electrons and ions, and L_c the discharge channel length. That is to say large enough to confine the electron in order to maximize the occurrence of ionizing collisions, but ineffective on ions trajectories. In addition the electron density shall be minimal in the anode vicinity in order to ensure the electric current continuity. Finally **E** field shall be as flat as possible in the exhaust plane to limit the plasma plume divergence. As a result the magnetic circuit shall be designed to create the suitable magnetic topology, i.e. a given radial induction gradient on the channel axis, a maximal radial magnetic component at the channel exit (Br_{max}), as well as an appropriate induction level and magnetic lens inclination in the exit plane.

Moreover the magnetic circuit constitutes the mechanical structure for the thruster. It provides reliable enough stiffness to absorb the high vibration levels and shocks occurring mostly during the ascent phase of the launcher.

The magnetic circuit represents about 70% of the thruster mass, therefore its mass reduction which is of great interest for the improvement of the thrusters competitiveness is also a big challenge.

2. Coils or electromagnets?

In a standard Hall thruster the magnetic field **B** is obtained with a set of coils, of poles and of magnetic screens. Their dimensioning requires particular attention to yield enough margins with regard to the magnetic saturation of

the ferromagnetic material. This saturation leads to insufficient performance of the magnetic circuit, a deficiency of electron confinement and in turn a decrease of the thruster performance.

Among all the advantages given by the use of permanent magnets, one may mention the reduction of the electrical power consumption, of the thruster size and mass, of the magnetic circuit heating and of cost.

A flight thruster being submitted to numerous thermal cycling the main drawbacks are the lack of knowledge about cycling and aging processes and their high sensitivity to temperature. A specific device was built to test magnets of different compositions, under severe temperature variations. The tests described in detail in Ref.3 aimed at evaluating the stability of the permanent magnet submitted to 8000 thermal cycles between -150°C and 600°C. A slight decrease of the remanence (less than 10%) was observed along the first 4000 thermal cycles with stabilization after. Finally, the test results showed that the magnets successfully verified the thermal specifications and enabled to validate the choice of permanent magnets for the present study.

II. The 1.5kW-class PPS®1350 HET

A. PPS®1350-G

1. Description

The PPS®1350-G is the Flight Model of the Snecma 1.5kW-class HET. The nominal operating point was chosen at discharge current *Id* and voltage *Ud* of 4.28 A and 350 V respectively. The thruster has been designed and manufactured by Snecma and has been both on ground and in-flight demonstrated[4] (Fig. 2).

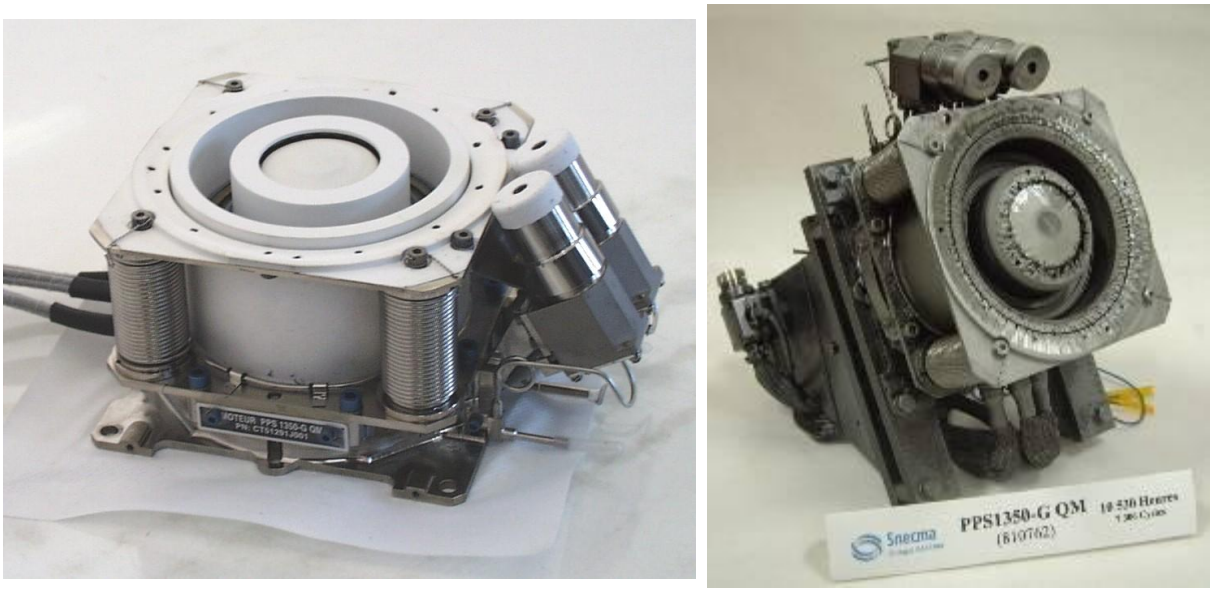

Figure 2. PPS®1350-G thruster at beginning of life and at end of life on its test support

During the thruster life test qualification achieved between 2003 and 2006 the thruster completed 10532h of operation and 7309 cycles with no decrease in performances during the whole lifetime. The thruster also ensured the success of the SMART-1 probe journey to the moon by achieving a world record of operation with 4960 h and about 800 cycles[5]; it covered more than 100 millions of km consuming only 82 kg of propellant (Xe).

2. Thruster performance

The thrust, efficiency and specific impulse (both including cathode flow rate) averaged along the lifetime are respectively of 89mN, 50% and 1650s at nominal operating point.

A wide characterization campaign was also achieved on an engineering model of the PPS®1350-G.[6] For a discharge voltage of 350V and a mass flow rate comprised in the [2.3-7.5mg/s] range the thrust and specific impulse were of [37-160mN] and [1500-2000s] respectively. Operated at twice the nominal power, three times the nominal discharge voltage and twice the nominal mass flow rate the thruster demonstrated thermal and electrical margins. Based on these considerations the magnetic topology of the PPS®1350-G flight model is considered as the reference one in the following.

B. PPS®1350 Technology Demonstrator

In order to evaluate new technologies, Snecma manufactured a 1.5 kW-class technology demonstrator of the PPS®1350-G model called PPS®1350-DT. The challenges and technological issues to be met for the implementation of new technologies on this thruster are discussed in detail in Ref.3. The PPS®1350-DT is designed to be dismantled in order to test new technological elements and materials and in turn assess their impact on the thruster behavior and performance. The objective is to test technologies for the next generation of HET designed by Snecma. The main modifications with regard to the flight model are related to the electrical configuration as well as the replacement of several parts of the thruster. For instance the anode / gas distributor can be changed to test other architectures or materials and the inner and outer rings of the discharge channel can be replaced. Concerning the magnetic circuit, internal, external and rear coil circuits are separated to enable to test several magnetic configurations. In addition the magnetic flux generators can be either permanents magnets or coils (Fig. 3).

All those modifications can be easily implemented.

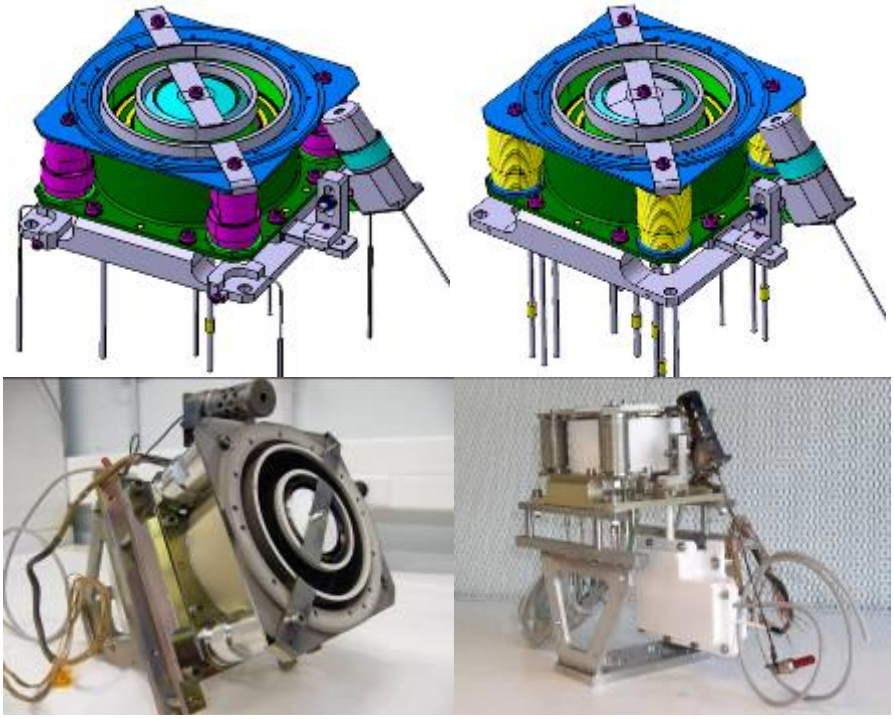

Figure 3. Sketches and pictures of the PPS®1350 DT models (left: with permanent magnets and right: with coils).

III. Magnetic topology

A. 2-D Magnetic modeling

Magnetostatic simulations were carried out with the Flux®2D finite-element software from Cedrat to design the magnets. The software simulates ferromagnetic materials with non linear and/or anisotropic permeabilities, coils as well as magnets. The main calculation steps are briefly described in the following.

1. Geometry

The PPS®1350-G reference thruster design, including the 4 external coils is modeled by a two-dimensional axi-symmetrical geometry[††]. Each asymmetrical part is basically modeled by an element of equivalent cross section.

The permanent magnets dimensioning consisted in optimizing their size. The parameters that could be varied in the study were the magnet section and height as well as the material magnetic characteristics.

[††]Comparisons between 3D and 2D modeling did not evidence much difference in the functional areas of the thruster, i.e. into the discharge channel and in the vicinity of the exit plane

2. Boundary conditions

The boundary conditions are of Dirichlet type on the thruster axis and of cyclic type at the infinity.

3. Physical properties

Each element is supposed isotropic with constant relative permeability μr.

The magnetic poles, screens and coil cores are made of standard Armco iron for which the magnetic characteristic is a spline curve depending on temperature. Figure 4 shows the plots provided by the Armco Company for 20°C and 500°C.

Permanent magnet are characterized by parameters strongly dependant on the material composition and on temperature. Generally for a given compound they decrease more or less as the temperature increases. And above a maximum temperature T_{max} some of the magnetic properties might be lost. The material for the magnets is a grade of samarium cobalt based alloy specifically chosen for its better performance during thermal cycles. The software inputs are the temperature dependent remanence *Brem* and permeability μr = 1,05.

Thermal simulations were carried out to estimate the magnet temperature in operation. With nominal operating parameters and coils current turned off a temperature of less than 550K was obtained.

4. Parameterization

The simulations were performed with magnetic characteristics of the materials at two extreme temperatures (293K and 573K or 750K depending on the thruster layout).

5. Post-processing

The maps provide the magnetic field lines and the induction levels. The main magnetic data (B_r/Br_{max} and lens inclination) are plotted along the channel axis, from near the anode exit plane up to few millimetres downstream of the channel exit plane. Quantitatively, the inclination of the magnetic field lines, defined as $arctan(B_z/B_r)$, is obtained by post-processing the axial (B_z) and radial (B_r) components of $\boldsymbol{B}$. A positive angle means that the normal to the magnetic field lines is tilted toward the thruster centerline and conversely.

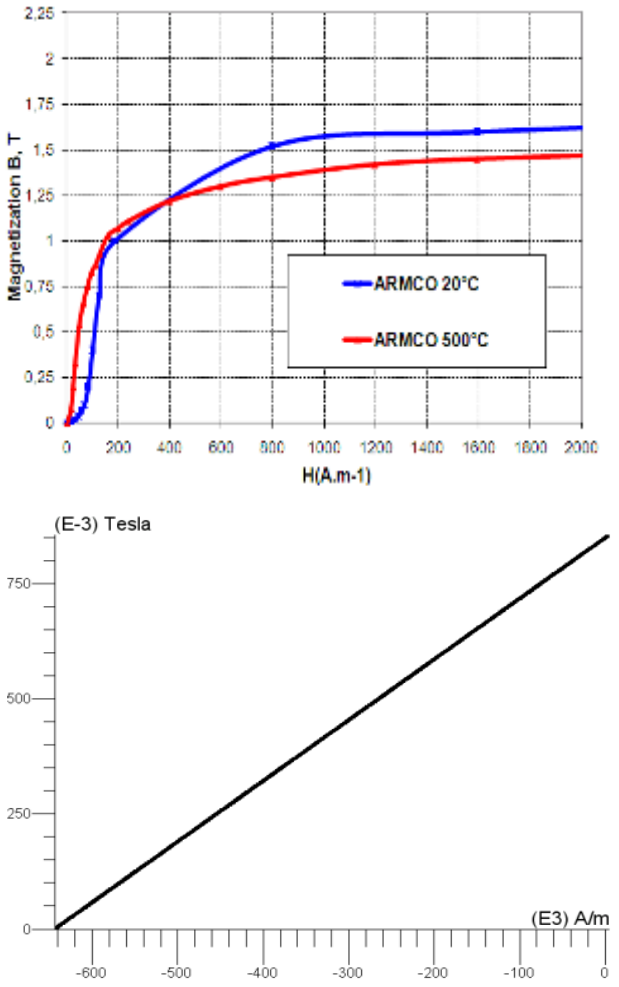

Figure 4. Magnetization as a function of the applied field. Above: Armco iron. Below: Magnets.

B. Measurements-Models Comparison

The parametric study on the magnet height, section and temperature, led to a design for the internal and the four external magnets. Their size was defined on the basis of the 2D modelizations that reproduces the magnetic topology as close as possible of the reference PPS®1350-G **B** field both in low and high temperature conditions. The calculated magnetic topology and lines in hot case are presented in Figure 5 for both configurations. It shows the magnetic distribution in the upper part of the channel and downstream of the channel exit. The maps as well as the lines are very similar with a few rare exceptions, in particular on the external channel wall. A high lens inclination is responsible for an increased flux of electrons and ions to the discharge channel walls and in turn for the erosion of the channel. At the intersection of the channel axis and the plane containing Br_{max} the inclination of the magnetic lines complies with positive and near zero values in both cases but slightly higher for the coil case. In ambient conditions this discrepancy is of about 1° versus about 2° in hot conditions. It means, in first approximation, that:

- The constant electric potential surfaces will be very similar in this area, and in turn the thruster performance will be comparable;
- Slightly lower ion and electron flux will impact the internal wall in the magnet case;
- The ion flux towards the walls will decrease during operation;
- The divergence is expected to be better in the magnet configuration;

- And as a result the thruster should not experience higher erosion or heating with magnets.

After manufacturing and thruster assembly two series of measurements were carried out, the first one in coil configuration, the second one in magnet configuration. They were performed with a specific set-up including a fixed mounting support for the thruster and a 3-axis magnetic probe. The probe is composed of 3 magnets sensors installed on a rotating-translating support enabling to scan the space domain in azimuthal, radial and axial directions. The measurements confirm the previous results.

The calculated and measured magnetic field evolutions on the channel axis are compared for both configurations in Figures 6 and 7. In order to facilitate the comparison, the results were divided by Br_{max} corresponding to the maximal radial component on the channel axis for the coil configuration in ambient conditions. Figures 6 a) and b) highlight the induction thermal stability in the coil configuration whereas in the magnet configuration the value decreases of about 10% at hot temperature. The coil configuration is less sensitive to temperature because the circuit was designed in order to provide sufficient margins with regard to saturation; as a result the remanence of the ferromagnetic material does not depend on temperature at first order. It follows that induction will decrease of less than 10% - in worst case - during operation up to magnet thermal stabilization. Owing the temperature sensitivity the magnets geometry was oversized at ambient temperature in order to compensate the drop at high temperature. But Figure 6 b) shows a discrepancy of maximum 6% between the calculated and measured induction levels in ambient conditions. It seems the model overestimated the results, which means the induction level will be less than expected in stabilized operation if the thruster reaches 573K.

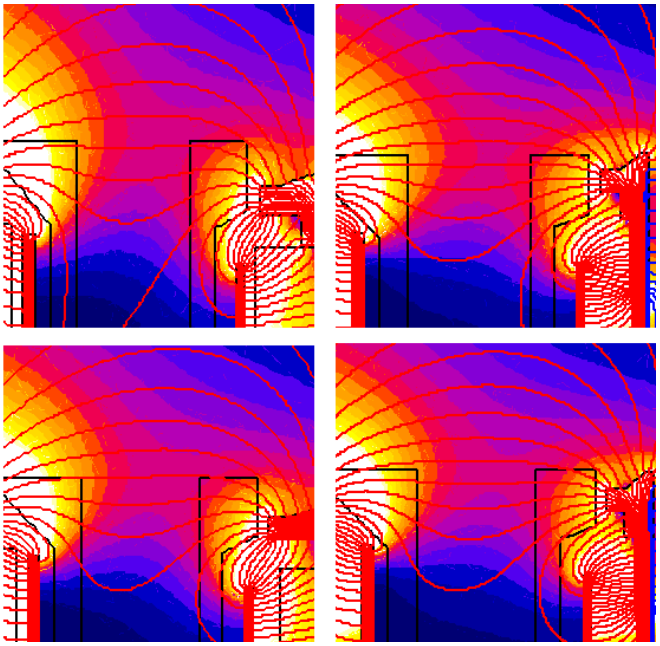

Figure 5. Results of the magnetostatic modelizations for the coil (left) and magnet (right) configurations. Above: ambient conditions; below: hot conditions.

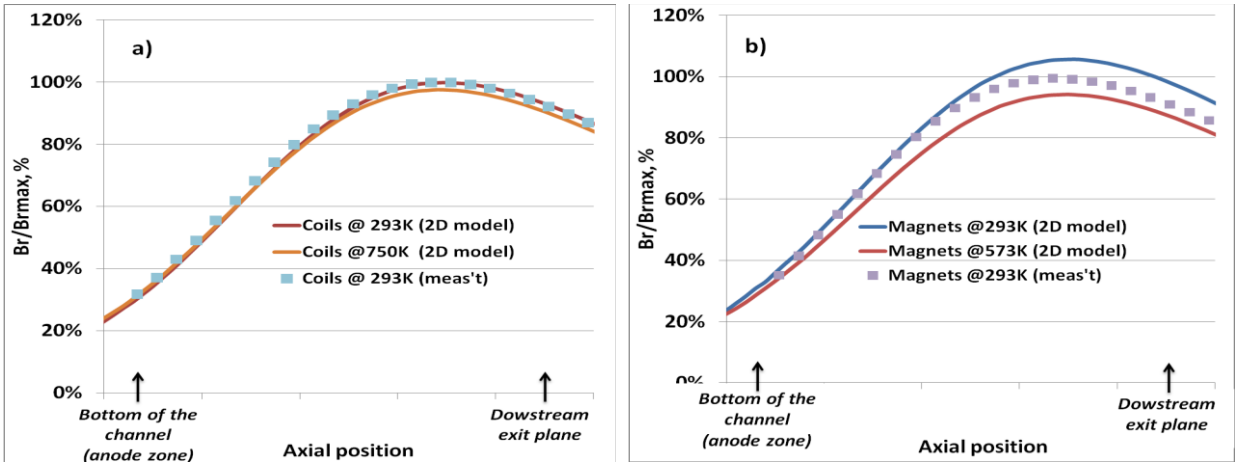

Figure 6. Evolution of the magnetic radial component on the channel axis (measurements and 2D modelizations) : a) for the coil configuration and b) for the magnet configuration for different temperatures

Figure 7 presents the comparison between the measurements for coils and magnets in ambient conditions. It highlights a very good similarity, with a relative difference lower than 0.5% in the area corresponding to the ionization and acceleration zones. Near the anode this difference increases but without exceeding 2.5%. The second

plot compares the modelizations in hot conditions: the previous relative differences become 1% and 2% respectively.

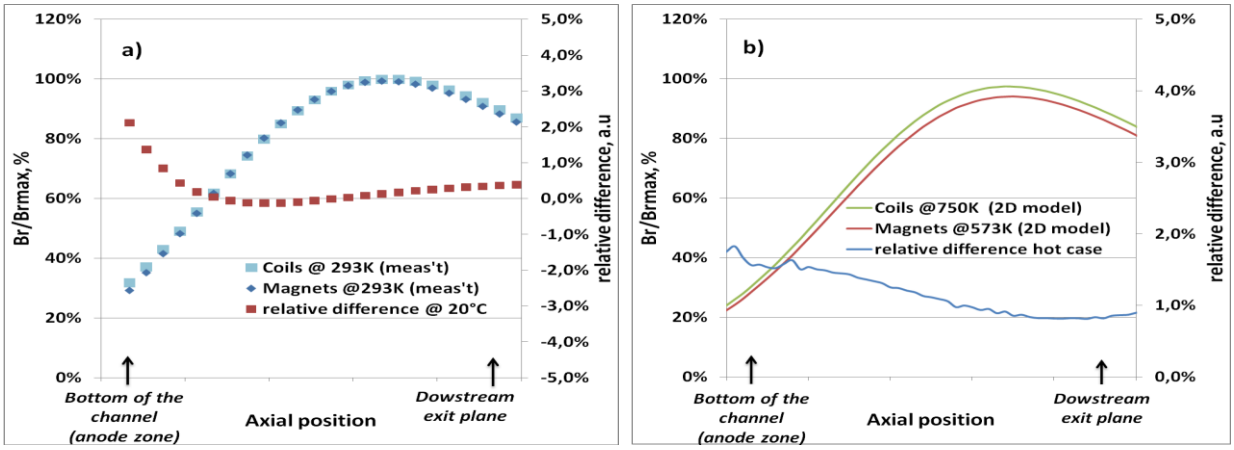

Figure 7. Comparison of the magnetic radial component evolution on the channel axis for both configurations. a) Measurements in ambient conditions and b) calculations in hot case

In a nutshell, this study clearly evidences the compliance of the measurements with the modelization results and shows that the behavior of the thruster may be affected, but in a slight way, in stabilized thermal conditions.

IV. Testing campaign

A. Description

A specific testing campaign was carried out with the demonstrator in coils and magnets configuration to assess the impact on the thruster performance. The tests were performed in LiB Snecma vacuum chamber designed to test HET for flight acceptance tests and for R&T activities. The main chamber is equipped with a pumping system enabling to reach less than 2.10^{-4} mbar during nominal operation. To characterize the thruster performance the bench was equipped with a thrust balance, and the divergence is calculated from measurements by Faraday probes installed on a rotating arm located 706mm downstream the channel exit plane. Current and oscillations were measured by Pearson410 and AP015 current probes and Fast Fourier Transform (FFT) calculated by a Lecroy oscilloscope. Temperatures were also controlled by the mean of an infra-red camera and a thermocouple installed on one of the thruster feet.

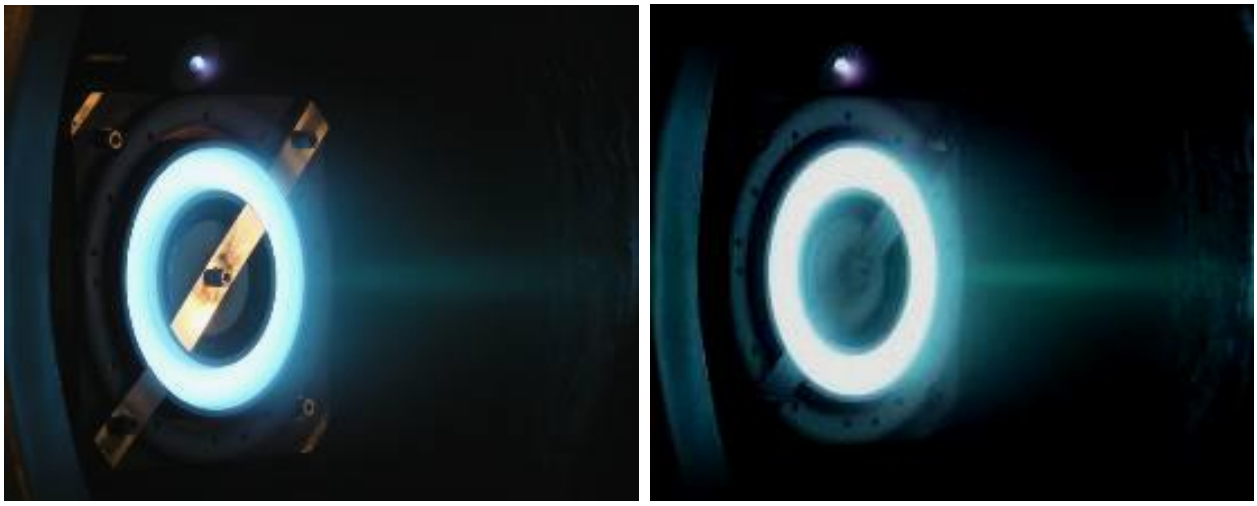

Figure 8. PPS®1350-DT thruster during operation (left: with permanent magnets; right: with coils).

The firing sequences consisted in performance tests around the nominal operating point (350V, 4.28A), and in high frequency measurements of the discharge current for different mass flow rates and discharge voltages. The first phase of the campaign was performed on the PPS®1350-DT in coil configuration, and the second one on the PPS®1350-DT in magnet configuration.

B. Performance comparison

Figure 8 shows pictures of the thruster at the nominal operating point for both configurations. Any visual difference was observed neither during ignition nor in stabilized regime. The plume discrepancies on the pictures are due to optical effects and different camera settings.

The performance assessment at nominal operating point is based on previous results obtained during the acceptance tests of two PPS®1350-G FM (Flight Model). Table 1 gathers the results after one hour of stabilized operation. It clearly shows compliance of the PPS®1350-DT - coil and magnet configurations - with the PPS®1350-G reference thruster, i.e. performance are in good agreement with those of a flight model.

Thruster model	Configuration	Ud	Id	Mass flowrate	Thrust	Isp	Thruster efficiency	Idosc	Ucrp	Divergence	Thrust vector longitude	Thrust vector latitude
		V	A	mg/s	N	s	%	A	V	degree	degree	degree
DT	Coils	351.4	4.28	5.23	91.2	1780	53.8	0.18	-19.2	44.7	0.34°	-0.57°
	Magnets	352.4	4.27	5.26	88.4	1713	49.4	0.29	-19.4	42.4	0.75°	-0.41°
FM002	Nominal cathode	351.4	4.28	5.20	92.7	1818	55.9	0.18	-16.4	40.5	-0.85	0.21
	Red't cathode	351.5	4.28	5.19	92.6	1818	55.8	0.18	-17.2	41.7	-1.07	0.12
FM004	Nominal cathode	351.4	4.28	5.29	91.4	1762	53.4	0.16	-17.0	40.1	0.33	0.34
	Red't cathode	351.5	4.28	5.25	90.4	1756	52.6	0.16	-18.1	40.7	0.24	0.32

Table 1. PPS®1350-DT performance at nominal operating point compared with FM (equipped with coils).

Nonetheless it shall be noted that the demonstrator presents performance slightly lower than the FM, whatever the configuration. In addition the coil configuration presents a little bit better performance than the magnet one except for the divergence.

Table 2 synthesizes the results of the second testing campaign that consisted in characterizing the performance box around the nominal operating point. FFT of the discharge current *Id* and of the discharge current oscillation level *Idosc* were also acquired during this phase: the magnet configuration presents higher levels of oscillation than the coil configuration. But again the obtained results are very satisfying with the same trend as previously.

	Ud (V)	Id (A)	Débit (mg/ sec)	F (mN)	Isp (sec	η (%)	Idosc (A)	Ucrp (V)
Coil configuration	352.9	3.86	4.81	80.0	1695	48.8	0.16	-19.1
	351.4	4.27	5.19	89.9	1768	52.8	0.18	-19.1
	350.8	4.50	5.39	97.7	1847	56.1	0.21	-19.1
	249.6	4.28	5.26	71.5	1385	45.5	0.24	-18.9
	351.4	4.27	5.21	91.2	1784	53.2	0.18	-19.1
	351.4	4.28	5.23	91.2	1780	53.8	0.18	-19.1
Magnet configuration	353.0	3.86	4.82	79.7	1688	48.4	0.26	-20.5
	352.4	4.27	5.26	88.4	1713	49.4	0.29	-19.4
	351.8	4.51	5.50	91.8	1703	48.4	0.29	-19.2
	371.4	4.28	5.25	91.0	1768	49.7	0.37	-19.4
	300.1	4.50	5.51	83.0	1536	46.3	0.26	-18.9
	299.2	5.00	6.03	92.3	1562	47.3	0.29	-18.1
	198.2	4.27	5.23	54.2	1057	33.2	0.16	-18.1

Table 2. PPS®1350-DT performance at different operating point in both configurations.

Figure 9 shows screenshots of the current oscillations and the signal FFT typically observed for low and high mass flow rates (around 3.5mg/s and 5mg/s). For low voltage *Idosc* is low, typically 0.2 A, and only the fundamental frequency is observed on the FFT. When the voltage increases, the discharge starts being more chaotic

Figure 9. Oscillation and FFT recorded at low (top) and high (bottom) mass flow rates. The discharge voltage increases from left to right.

alternating high and low levels of oscillations. At high voltage the discharge current FFT presents the fundamental frequency and its harmonics. *Idosc* increases then up to 1.5 to 2 A.

All these results are discussed in the next paragraph.

C. Discussion

The lower performance obtained with the demonstrator equipped with permanent magnets with regard to the coil configuration, and also both with reference thrusters, are mainly due to a slight difference in the magnetic topologies.

The specific magnetic configuration of the flight model aiming at lowering the magnetic field in the anode zone explains the difference. Moreover magnetic field was undersized in ambient conditions however the magnet temperature was actually lower than expected, around 450K maximum versus 550K taken for the magnet sizing. This leads to an induction level larger than expected, which compensates the error generated by the 2D model. Taking that into account, we can estimate a discrepancy of about 6% on Br_{max} with regard to coils which can also have an impact on the thruster efficiency.

Moreover the magnetic topologies were calculated for the same temperature of the internal and external magnets but the external magnets are most probably around 40K colder than the internal one because they can more easily

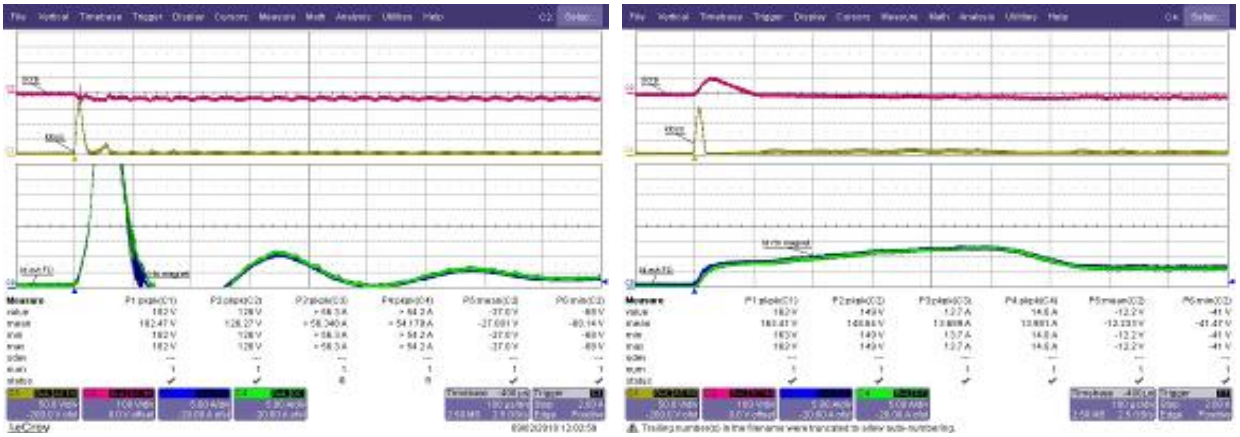

Figure 10. Oscillation and FFT at ignition (left: magnet configuration; right: coils configuration)

evacuate thermal loads by radiation. The positive consequence is the modification of the lens inclination that explains the reduction of divergence in magnet configuration.

Finally inrush currents during ignition were more violent for the magnet configuration (Fig. 10). The suppression of the coils in the discharge current electric circuit explains this trend: in the standard configuration the coils also enables to damp current peaks.

V. PPS®1350 Optimization

A. Magnetic optimization

Tests performed in magnet configuration show very similar performance with standard configuration. In addition the thermal cycling carried out on magnets samples did not evidence critical points with regard to aging. Based on these considerations the implementation of magnets on the PPS®1350-G was further assessed, with mass optimization as the main driver of the study.

On the PPS®1350-DT the magnets were placed at the same location than the coils but their section was lower, which offers the possibility to move it closer to the thruster axis and thus to reduce the magnetic front plate overall dimension. Therefore less magnetic losses are generated and the magnet section can be reduced further. It is then possible to move them closer, and so on. And little by little the modifications affect the magnet, the magnetic circuit and the thruster mounting support. The impact on the overall mass of the thruster was already illustrated by the mass optimization study achieved on the PPS®5000, a 5kW-class thruster under development in Snecma: the study enabled to save more than 25% of the total mass.

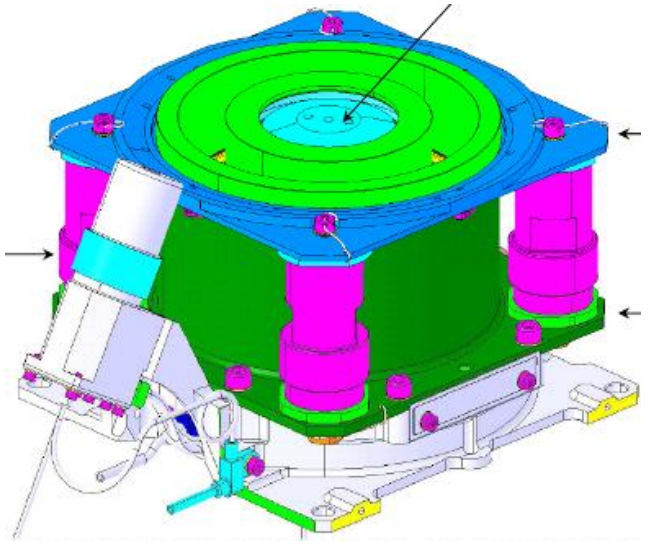

Figure 11. Preliminary design of the permanent magnet PPS®1350

Modelizations are performed at each step using Flux®2D software. In order to guarantee the respect of the magnetic configuration, the size and shape of most of the magnetic elements were modified. Finally the preliminary design of a permanent magnet thruster optimized for mass was obtained: it enables to save 12% of the total mass (3.86 kg *vs.* 4.42 kg). Figure 11 presents the optimized thruster with only one cathode but the mass saving was calculated from the anode block point of view.

B. Further improvements

For the next generation of commercial communications satellites, HETs simplifications are of real interest because of international concurrence and cost-constraints. Based on this successful campaign, further activities are in progress with the objective of improving the thruster competitiveness. For instance, a testing campaign will be in the immediate future dedicated to assess the performance of several grades of ceramic materials for the discharge chamber. On another hand further technical simplification are proposed such as the suppression of one cathode and one XFC, on the base of the PPS®1350-S, which was first proposed and selected in 1999 for the *Skybridge* program. Recent tests demonstrated the cathode cross firing feasibility, i.e. in a two thruster configuration such as on a TMA-NG[7]. Thrusters can be operated with any of the two cathodes, *i.e.* its own one or the cathode of the other thruster, and respectively.

VI. Conclusion

Hall Effect Thrusters are considered today as the most promising propulsive systems for station keeping and attitude control of geostationary commercial satellites. For the next generation of HETs, broadened operating capabilities are of interest but require the development of innovative technologies. Snecma manufactured a 1,5 kW-class demonstrator thruster called PPS®1350 DT. This HET was built to be dismantled in order to assess

technological modifications. A testing campaign implemented magnets instead of coils to generate the magnetic field. Owing the good performance of the thruster, the PPS®1350-G magnetic topology was chosen as reference for the magnet sizing.

Globally the testing campaign is a success: performance is as expected. Efficiency and thrust are slightly better for the coil configuration; it is due to magnetic topology which is not exactly the same in both cases.

The study highlights that the impact of using permanent magnets instead of electromagnets to generate the magnetic field is very significant, especially in terms of simplification and power consumption lowering (electric circuit), thermal loads decrease (minus 50-100K on the magnetic circuit), mass savings (-12%) and in turn cost reduction. Implementation of permanent magnets instead of coils to generate the magnetic field is thus an interesting option for the improvement of the PPS®1350-G competitiveness.

Acknowledgments

The PPS®1350-DT activities are performed through CNES and Snecma internal supports.

References

[1] Marchandise et al, "Compact Hall Effect Assembly Propulsion subsystem PPS®X00, first test results in the range 300W-500W", *32nd International Electric Propulsion Conference*, IEPC-2011-xxx, 2011

[2] Zurbach et al, "Performance evaluation of a 20 kW Hall Effect Thruster", *32nd International Electric Propulsion Conference*, IEPC-2011-xxx, 2011. 2011

[3] Zurbach et al, "The PPS®1350 DT: a HET Model for permanent magnet and new ceramic evaluation", *xx International Space Propulsion Conference*, ISPC-2008-xxx, 2008

[4] Cornu et al, "The PPS®1350-G Qualification Demonstration: 10500 hrs on the Ground and 5000 hrs in Flight", *43rd Joint Propulsion Conference*, AIAA-07-5197, 2007

[5] Koppel, C.R., et al, "The SMART-1 Electric Propulsion Subsystem around the Moon: In Flight Experience," *41st AIAA/ASME/SAE/ASEE Joint Propulsion Conference*, Tucson, Arizona , AIAA 2005-3671, 2005

[6] Prioul, M., et al., "PPS®1350 Qualification Status and Performance," *3rd International Space Propulsion Conference*, Chia Laguna, Italy, ESA SP-555, 2004.

[7] Lorand et al, "Next Generation of Thruster Module Assembly (TMA-NG)", *32nd International Electric Propulsion Conference*, IEPC-2011-201, 2011